Applied Geochemistry 27 (2012) 2335–2347

Contents lists available at SciVerse ScienceDirect

Applied Geochemistry

journal homepage: www.elsevier.com/locate/apgeochem

Evolution of the chemistry of Fe bearing waters during CO_2 degassing

J.N. Geroni [a,*], C.A. Cravotta III [b], D.J. Sapsford [a]

[a] Cardiff School of Engineering, Cardiff University, Queen's Buildings, The Parade, Cardiff CF24 3AA, UK
[b] U.S. Geological Survey Pennsylvania Water Science Center, 215 Limekiln Road, New Cumberland, PA 17070, USA

ARTICLE INFO

Article history:
Received 23 February 2012
Accepted 23 July 2012
Available online 2 August 2012
Editorial handling by R.B. Wanty

ABSTRACT

The rates of Fe(II) oxidation and precipitation from groundwater are highly pH dependent. Elevated levels of dissolved CO_2 can depress pH and cause difficulty in removing dissolved Fe and associated metals during treatment of ferruginous water. This paper demonstrates interdependent changes in pH, dissolved inorganic C species, and Fe(II) oxidation rates that occur as a result of the removal (degassing) of CO_2 during aeration of waters discharged from abandoned coal mines. The results of field monitoring of aeration cascades at a treatment facility as well as batchwise aeration experiments conducted using net alkaline and net acidic waters in the UK are combined with geochemical modelling to demonstrate the spatial and temporal evolution of the discharge water chemistry. The aeration cascades removed approximately 67% of the dissolved CO_2 initially present but varying the design did not affect the concentration of Fe(II) leaving the treatment ponds. Continued removal of the residual CO_2 by mechanical aeration increased pH by as much as 2 units and resulted in large increases in the rates of Fe(II) oxidation and precipitation. Effective exsolution of CO_2 led to a reduction in the required lime dose for removal of remaining Fe(II), a very important factor with regard to increasing the sustainability of treatment practices. An important ancillary finding for passive treatment is that varying the design of the cascades had little impact on the rate of CO_2 removal at the flow rates measured.

1. Introduction

Iron is the most abundant transition metal in the Earth's crust. It occurs in numerous minerals including goethite (FeOOH), haematite (Fe_2O_3), magnetite (Fe_3O_4), pyrite (FeS_2), and various ferromagnesian silicates (olivine, augite, hornblende) and, because of mineral weathering, is a common dissolved constituent in groundwater and mining-influenced water around the world (Kothari, 1988; Moncur et al., 2009; Nordstrom, 2011). Elevated concentrations of dissolved Fe can degrade the aquatic environment and contaminate water supplies (Carter et al., 1996; Lucassen et al., 2000; DeNicola and Stapleton, 2002). The removal of Fe from ferruginous waters adds to the costs of mining and of treating wastewater and potable water supplies by utility companies.

Current practices for the removal of dissolved Fe(II) often require lime dosing to raise pH or the addition of chemical oxidants to covert the Fe(II) to relatively insoluble Fe(III) solids (Faust and Osman, 1998; Coulton et al., 2003; Jarvis et al., 2003). Critical drivers for the water industry in the UK (and elsewhere) include reagent and energy reduction which is leading to a reappraisal of these standard removal technologies. Thus, the potential for CO_2 removal (degassing) to increase pH and decrease reagent demand is of interest to numerous stakeholders. Questions are frequently asked such as what is the best design for CO_2 degassing, what is the required residence time and how can passive technologies such as aeration cascades best be used to make savings in energy and chemical consumption? Furthermore, CO_2 degassing can be important in wastewater treatment by increasing pH and inducing the precipitation of $CaCO_3$ and struvite which might otherwise encrust pumps and distribution systems (Larson and Buswell, 1942).

Ferruginous waters are common in coal mining areas. The high concentrations of dissolved Fe(II) can result from the oxidation of pyrite and other Fe-bearing sulphide minerals in aerobic environments or the reductive dissolution of goethite and other hydrous ferric oxide (HFO) minerals in anaerobic environments (Langmuir, 1997). The oxidation processes are acid generating, but for many coal mine waters, a combination of limestone dissolution and, in some cases, SO_4 reduction or HFO reduction coupled with the oxidation of organic C results in a circumneutral pH at the point of discharge (Langmuir, 1997). Because CO_2 is a product of reaction with limestone or the oxidation of organic C, the emerging waters frequently are supersaturated with respect to atmospheric CO_2 (Langmuir, 1997; Rose and Cravotta, 1998; Kirby and Cravotta, 2005b). This results in a natural driving force for degassing of CO_2 over time as the exposed ground water approaches equilibrium with the atmosphere. In some instances, deep mine waters that are pumped to the surface contain further excess CO_2 under pressure and can be observed to effervesce on emergence in the same way as naturally carbonated mineral waters.

* Corresponding author. Tel.: +44 (0)7971 087398.
E-mail address: geronijn@cf.ac.uk (J.N. Geroni).

0883-2927/$ - see front matter © 2012 Elsevier Ltd. All rights reserved.
http://dx.doi.org/10.1016/j.apgeochem.2012.07.017

In addition to the problems faced by the water and mining industries, Fe(II) is a common groundwater contaminant in many developing countries where aesthetic concerns can lead to the rejection of pumped water in favour of unsafe surface sources (Carter et al., 1996). It is therefore a critical public health issue to reduce the Fe(II) concentration and increase the local acceptance of the groundwaters. In this paper, CO_2 degassing from ferruginous mine water discharges is studied with the goal of improving the design of mine water treatment systems and reducing the impact of ferruginous waters on the environment and economy.

1.1. Chemistry of Fe(II) oxidation and CO_2 degassing

On exposure to atmospheric O_2, Fe(II) spontaneously oxidises to Fe(III), which then precipitates to form HFO solids at circumneutral pH according to Eqs. (1) and (2) (Langmuir, 1997; Rose and Cravotta, 1998). These oxidation and subsequent precipitation reactions are the key steps involved in the removal of Fe from ferruginous waters.

$$Fe^{2+} + \frac{1}{4}O_2 + H^+ \rightarrow Fe^{3+} + \frac{1}{2}H_2O \quad (1)$$

$$Fe^{3+} + 3H_2O \rightarrow Fe(OH)_{3(S)} + 3H^+ \quad (2)$$

Within the circumneutral pH range, the rate of Fe(II) oxidation can be described as a homogeneous process (involving only dissolved Fe(II) species) by Eq. (3) (Stumm and Morgan, 1996). The second order dependence on $[OH^-]$ means that the time required for the successful treatment of ferruginous water is highly pH dependent, with Fe(II) having a half life of seconds at pH 8 and weeks at pH 5. An increase in pH of 1 unit results in an increase in oxidation rate of 2 orders of magnitude.

$$-\frac{d[Fe(II)]}{dt} = k_1[Fe(II)][OH^-]^2P_{O_2} \quad (3)$$

Since pH is the most significant variable affecting the homogeneous rate of Fe(II) oxidation, it is important to have an understanding of the processes that affect pH in ferruginous waters. Groundwaters commonly contain elevated levels of dissolved CO_2 compared to surface waters that are at equilibrium with the atmosphere (Langmuir, 1997). Circumneutral groundwaters also contain elevated levels of dissolved carbonates and bicarbonates, referred to in this context as alkalinity because of the acid-neutralising capacity of $CaCO_3$ (Stumm and Morgan, 1996). Elevated levels of dissolved CO_2 also add to the acidity and depress the pH according to Eqs. (4) and (5) (Kirby and Cravotta, 2005a,b; Kirby et al., 2009).

$$CO_{2(aq)} + H_2O \rightarrow H_2CO_3 \quad (4)$$

$$H_2CO_3 \leftrightarrow HCO_3^- + H^+ \quad (5)$$

Generally, the pH of groundwater will increase as the CO_2 exsolves to the atmosphere; however, the oxidation and hydrolysis of Fe(II) (Eqs. (2) and (3)) may cause the pH to decrease. The evolution of pH is governed by the balance between alkalinity, the acidity due to dissolved CO_2, and the acidity due to the hydrolysis of dissolved Fe, Mn and other metals (Kirby and Cravotta, 2005a,b). Mine waters having total alkalinity greater than total acidity are termed 'net-alkaline' and are often considered to be 'self-treating,' i.e., do not require the addition of chemicals to maintain circumneutral pH after complete oxidation and hydrolysis of the dissolved Fe and Mn. Waters having acidity greater than alkalinity are termed 'net-acidic' and generally require the addition of alkali or lime in order to maintain or raise pH to near neutral values and achieve acceptable Fe removal rates (Younger et al., 2002; Kirby and Cravotta, 2005a,b).

Aeration cascades are commonly included at mine water treatment sites for the introduction of dissolved O_2 (DO) that is required for Fe(II) oxidation (Younger et al., 2002; PIRAMID, 2003). In addition to increasing DO, these structures promote the degassing of excess dissolved CO_2, which has been recognised as important for conventional water treatment applications (Stumm and Morgan, 1996) and is increasingly recognised as important for the efficient treatment of ferruginous waters (Cravotta, 2007; Kirby et al., 2009). However, the dissolution (ingassing) rate of O_2 generally is faster than the exsolution (degassing) rate of CO_2 because, in addition to being a dissolved gas, CO_2 forms dissolved carbonate species and associated ion complexes (Stumm and Morgan, 1996; Langmuir, 1997; Kirby and Cravotta, 2005b; Kirby et al., 2009).

1.2. This study

This paper evaluates the evolution of water chemistry with respect to Fe, pH, alkalinity and carbonate/bicarbonate speciation as a consequence of aeration and CO_2 degassing. The study uses data collected from batch experiments conducted in the field at two net alkaline and three net acidic ferruginous coal mine discharges in the UK. Commensurate aims of this paper were to document the efficiency of degassing of CO_2 and the corresponding effects on Fe(II) removal by different designs of cascade and mechanical aeration. Design considerations with respect to the inclusion of aeration stages in the passive and active treatment of ferruginous groundwaters and mine waters are discussed in the context of CO_2 degassing, pH changes, and the optimisation of Fe(II) oxidation rates.

2. Methods

2.1. Aeration cascade experiments

All aeration cascade experiments were carried out at the Strafford underground coal mine site in England (Fig. 1). The mine water is circumneutral with low Fe concentration and is pumped to a single point at the top the set of aeration cascades. The aeration cascades during this study (Fig. 2) were split into two sections of the same width and total height. Stop logs were used to divert the flow of water down one or other of the cascades channels.

Five cascade configurations with various numbers of steps and plunge pools were tested as shown in the schematic diagram (Fig. 3). Configuration (1) was set up by extending a wooden board across the middle section of the cascades to create one long drop to the distribution channel beneath. Weir boards attached to the front of the steps and stop logs in the distribution channel were used to create the plunge pools in configurations (2b and 3b) (Fig. 3). Configurations 2a and 2b were situated on the left hand section in the photograph in Fig. 2a, with 3a and 3b in the right hand section. The total drop across all of the cascade configurations was 2200 cm. Weir boards were uniform in height across the entire width of the cascades (i.e. not v notch, triangular, etc.). Each cascade design was run alone as indicated in Fig. 2a.

Four Hanna HI 9828 handheld multiparameter meters were used to log pH, dissolved O_2 (DO) and temperature at the top and bottom of the aeration cascades. The meters were calibrated daily and were programmed to record values at 10-s intervals for the duration of logging. The meters were used in pairs at the top and bottom of the cascade and swapped during the day so that each meter logged readings at both the top and bottom of the cascade for a minimum of 2 h on each day. Logging occurred for 4–5 h

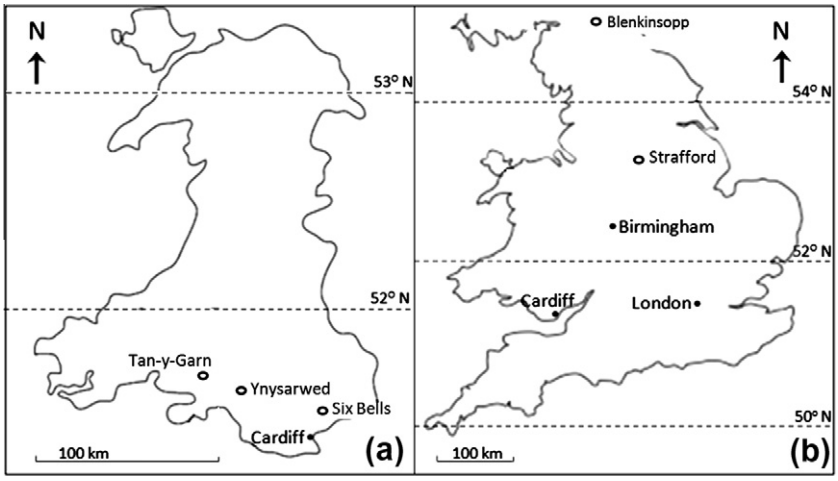

Fig. 1. Location of mine waters used in this study (a) in Wales, (b) in England (unfilled circles).

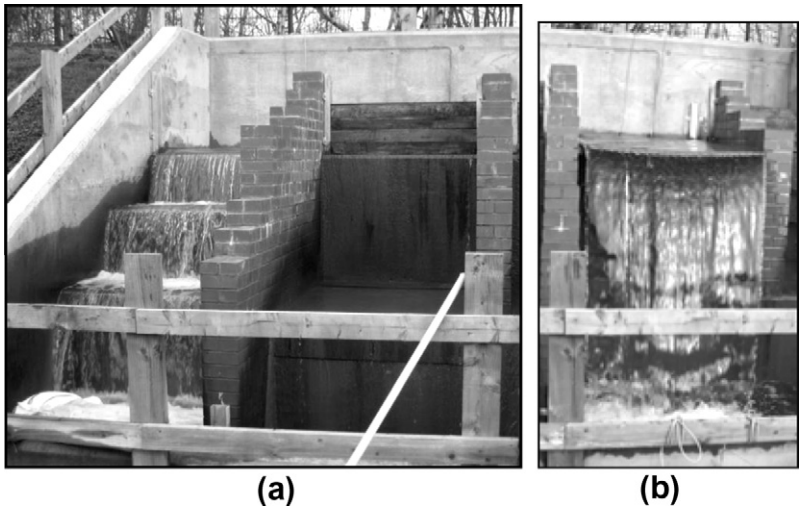

Fig. 2. Aeration cascades at the Strafford mine water treatment site showing (a) stepped cascades and (b) modification to single drop (waterfall) design.

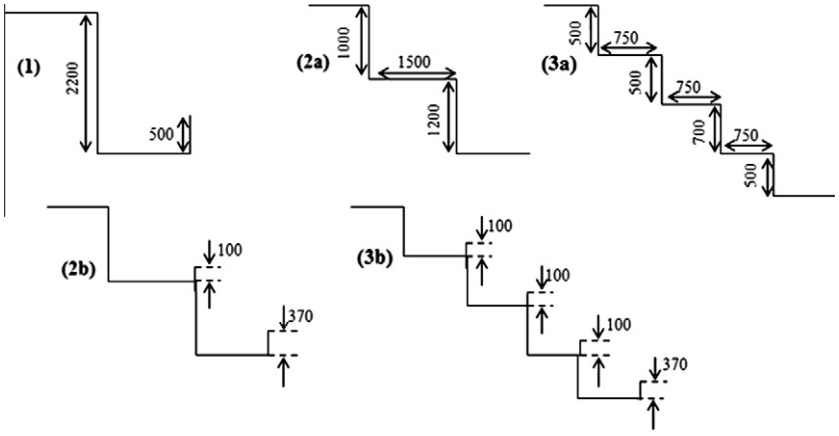

Fig. 3. Cascade configurations. All measurements in mm, all cascades 1275 mm wide.

for each of the configurations tested. Paired readings for each of the logged parameters were then averaged to produce the values reported; pH values were converted to H^+ concentration before averaging and then converted back to pH. Flow rates were also recorded continuously by inline sensors in the pumping house at the site. During the entire period studied the flow was within the range 29–30 L/s.

2.2. Batchwise CO_2 stripping experiments

Batchwise aeration experiments were conducted at three abandoned underground coal mines in Wales (Tan-y-Garn, Ynysarwed and Six Bells) and one abandoned underground coal mine (Blenkinsopp) in England (Fig. 1). Tan-y-Garn, Ynysarwed and Blenkinsopp all had marginally net acidic waters and Six Bells had net alkaline water. All of the sites currently have treatment schemes operated by the UK Coal Authority which comprise wetlands and settling lagoons as well as a Reducing Alkalinity Producing System (RAPS) at Tan-y-Garn and caustic soda dosing at Blenkinsopp. At each of these sites, approximately 15 L of freshly emerged mine water was taken in a bucket and mixed and aerated using a battery powered pump which created a fountain like effect within the bucket (air was not bubbled through the water). Mixing/aeration was carried out for 2 h at the net acidic sites and just over 30 min at Six Bells (net alkaline). All experiments were carried out in duplicate. The pH, temperature, and DO were logged at 10-s intervals using two Hanna HI 9828 handheld multiparameter meters. Both meters were calibrated daily prior to experimentation.

2.3. Water quality measurements

Samples for Fe and alkalinity measurements were collected at the top and bottom of the aeration cascades for each of the configurations studied (4 h after logging started). The samples at the bottom of the cascades were taken from the entrance to the distribution weir ahead of the first settling lagoon. Water samples were also taken at the outlet from the settling ponds shown in Fig. 4. Likewise, samples for Fe and alkalinity were collected at the beginning and end of each CO_2 stripping experiment. For dissolved Fe(II) analysis, 15 mL samples of the fresh and aerated mine water were immediately filtered through 0.8/0.2 μm Acrodisc PF syringe filters with Supor membrane and acidified with four drops of 10% HNO_3 to quench the Fe(II) oxidation reaction. Unfiltered samples for total Fe determination were also collected at Strafford. Dissolved Fe(II) and total Fe concentrations were determined in the laboratory by ICP-OES. The assumption was made that all Fe passing a filter with 0.2-μm pore size was dissolved Fe(II) as Fe(III) hydroxide precipitates form extremely quickly at circumneutral pH and would, therefore, be removed by the filter. Control experiments demonstrated the preservation of Fe(II) in split samples acidified with HNO_3 or HCl.

Alkalinity in100 mL samples of fresh and aerated mine water was measured on site using a Hach digital titrator with a 1.6 N H_2SO_4 cartridge and bromocresol green methyl red indicator. The titration end point was indicated as a colour change from green to pink, which corresponds to an approximate end point of pH 4.5. Acidity in100 mL samples of fresh and aerated mine water was also measured on site using a Hach digital titrator with a 1.6 N NaOH cartridge to an end point of pH 8.4. Additionally "hot acidity" was titrated in the field to determine net-acidity/net-alkalinity as described in APHA (1998).

2.4. Calculating changes in dissolved CO_2 and Fe(II) concentration

2.4.1. Aeration cascades

Values for dissolved CO_2 concentration in the untreated and aerated water samples were calculated from alkalinity, temperature and pH with PHREEQCi geochemical speciation software (Parkhurst and Appelo, 1999). Averaged data for temperature and pH (calculated by converting measured pH values to H^+ concentration then averaging before converting back to pH) recorded on the paired meters were used to give a single value for dissolved CO_2 at the top and the bottom of the cascades.

2.4.2. Batchwise experiments

A spreadsheet based 4th order Runge–Kutta (RK4) model was used initially to compute the concentration of residual Fe(II) as a function of elapsed time based on Eq. (3) (Stumm and Lee, 1961; Stumm and Morgan, 1996). Values input into the model were initial Fe(II) concentration along with the average values of pH, temperature, and DO for each 10-s interval logged throughout the experiments. The apparent value for the homogeneous Fe(II) oxidation rate constant ($k_1^* = 1.33 \times 10^{12}$ to 1.33×10^{14} M^{-2} atm^{-1} s^{-1}) for each experiment was chosen to yield the residual Fe(II) at the end of the experiment. These apparent rate constants were a factor of 1–100 times the reference value of 1.33×10^{12} M^{-2} atm^{-1} s^{-1} at 20 °C (Stumm and Morgan, 1996, p. 683) and were within the range of previous estimates for Fe(II) oxidation rates in ferruginous mine waters (Geroni and Sapsford, 2011).

Alkalinity measured for the fresh mine water was assumed to be consumed according to the stoichiometry of Eq. (6). Decreases in alkalinity over time were calculated as a function of the estimated decreases in Fe(II) concentration (this method has been used previously by Kirby et al., 2009). Finally the calculated values for Fe(II) and alkalinity together with the logged values for pH and temperature were input into PHREEQCi to calculate changes in dissolved inorganic C speciation over time.

$$Fe^{2+} + 2HCO_3^- + \frac{1}{2}H_2O + \frac{1}{4}O_2 \rightarrow Fe(OH)_3 + 2CO_2 \quad (6)$$

To facilitate the evaluation of the interactions among the initial alkalinity, pH, and Fe(II) oxidation rate, the major carbonate speciation equations and thermodynamic constants from the PHREEQCi data base were added to the spreadsheet with the RK4 model. The spreadsheet estimates of carbonate speciation, including estimated

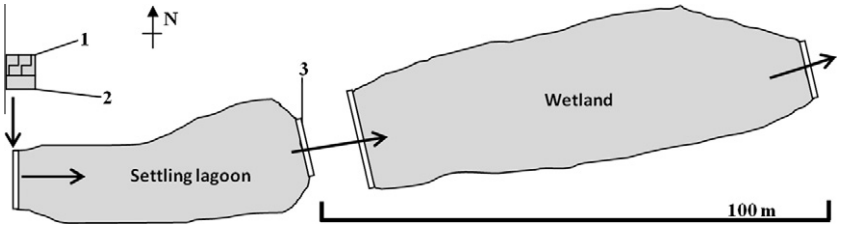

Fig. 4. Schematic diagram of the Strafford mine water treatment site. Numbered sampling points for aeration cascade experiments are marked. Direction of flow of water indicated by arrows.

partial pressure of CO_2 (P_{CO_2}) on the basis of Eqs. (4) and (5), were consistent with results obtained with PHREEQCi. The computed changes in the P_{CO_2} were then used to quantify the rate of CO_2 degassing during the aeration experiments. The rate of CO_2 degassing was evaluated considering both 1st and 2nd order asymptotic exponential models (Langmuir, 1997; Cravotta, 2008), with the latter providing a better fit of the empirical data (Geroni, 2011). The integrated form of the 2nd order rate equation is shown as Eq. (7), where C_s is the steady state (equilibrium) value, C_o is the initial value and C_t is the value at time t for the negative logarithm of P_{CO_2} in atmospheres (pCO_2). Values for $-k_La$ (the mass transfer coefficient) were calculated from the linear slope estimate of $[1/(C_s - C_t) + 1/(C_s - C_o)]$ versus t over the first 10–25 min of the experiments. The value of C_s was varied to yield k_La that approximated the trend for P_{CO_2} (C_t) during each experiment. The modelled values of C_s ($P_{CO_2} = 10^{-3.4}$–$10^{-1.7}$ atm) and k_La for the batch aeration experiments were consistent with previous aeration studies of ferruginous coal mine drainage indicating initially rapid CO_2 degassing and approach to a steady state that can be at disequilibrium with atmospheric CO_2 (Cravotta, 2007; Kirby et al., 2009).

$$t \cdot k_La = \frac{1}{(C_s - C_t)} + \frac{1}{(C_s - C_o)} \quad (7)$$

A second kinetic model was built using PHREEQCi to couple the rate equations for Fe(II) oxidation and CO_2 degassing and calculate the changes in pH and corresponding changes in concentrations of Fe(II) and dissolved inorganic C species over elapsed time. The model was adapted from previous work by Cravotta (2007). Values for pH, alkalinity, DO, and Fe(II) concentration measured at the start of the experiments and the average temperature during the experiments were input along with estimated k_La (calculated for the 2nd order rate equation) and apparent k_1 values (as used in the RK4 model). Model calibration was conducted to obtain the best fit of the measured data for logged pH (paired values) and the measured values for alkalinity and Fe(II) at the beginning and end of each batchwise CO_2 stripping experiment. Apparent values of the Fe(II) oxidation rate, k_1^*, for model calibration were estimated by multiplying the reference k_1 value of 1.33×10^{12} M^{-2} atm^{-1} s^{-1} at 20 °C (Stumm and Morgan, 1996, p. 683) by a factor ranging from 0.1 to 100, consistent with prior work (Geroni and Sapsford, 2011). Likewise, to match the observed data, values of C_s ranging from P_{CO_2} of $10^{-1.7}$ to $10^{-3.4}$ atm were evaluated to estimate representative k_La values for each experiment.

3. Results

3.1. Aeration cascade performance

The emergent groundwater at the Strafford site was suboxic (DO < 1 mg/L) and net alkaline (520 mg/L as $CaCO_3$), with pH of 6.6–6.8 and Fe(II) concentration of 5 mg/L. Measurements showed that DO was approaching saturation across all of the cascade configurations with no appreciable variation between the different designs. This was in line with previous work conducted at a number of other mine water treatment sites in South Wales which showed that cascades of varying height and length were successful in encouraging O_2 saturation (Geroni et al., 2009; Sapsford and Pugh, 2010).

Table 1
Changes in pH and computed total CO_2 across the cascades at Strafford.

	pH			Dissolved CO_2 (mg/L)		
	Top	Bottom	Change	Top	Bottom	Change
1	6.5	7.0	0.5	352	126	266
2a	6.6	6.8	0.2	317	200	117
3a	6.8	7.0	0.2	200	126	74
2b	6.7	7.2	0.5	252	59	193
3b	6.7	7.0	0.3	252	126	126

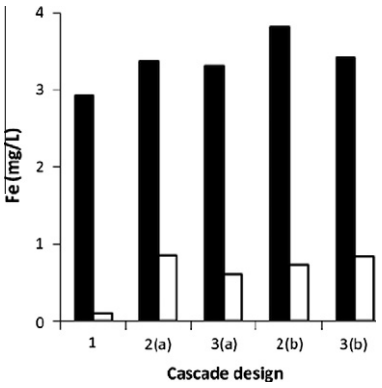

Fig. 5. Measured Fe concentrations at outlet of first settling lagoon at Strafford (sampling point 3 in Fig. 4) Total Fe (black) and Fe(II) (white).

The results for pH change over the aeration cascades as well as changes in dissolved CO_2 calculated using PHREEQCi are shown in Table 1. The changes in pH were small (0.2–0.5) and did not show any recognisable variation with changing cascade design (Table 1). Alkalinity concentrations at the top and bottom of the aeration cascades were the same, within experimental error varying by ±5 mg/L, so the same alkalinity value of 520 mg/L $CaCO_3$ equivalent was used for all calculations of dissolved CO_2 concentration. Nevertheless, the small increases in pH corresponded to relatively large changes in the concentration of dissolved CO_2 of the order of 100–200 mg/L which equated to a change of 37–64%. Despite the increased DO and pH, there was no measureable change in Fe(II) concentration between the top and bottom of the aeration cascades for any of the designs. Temperature was consistent at 13.0 °C throughout. It should be noted that the errors in calculation of changes in dissolved CO_2 concentration are potentially high as a result of uncertainty in the measurements. Further repetition of the aeration cascade design experiment at different sites could provide more conclusive results.

Measurements taken at the end of the first settling lagoon (sample point 3 in Fig. 4) showed that overall Fe removal rates were also not considerably impacted by changes in the aeration cascade design. The lagoon had a residence time of approximately 17 h and samples were taken after 24 h of operation for each cascade design. A summary of the Fe(II) (0.2 μm filtered samples) and total Fe data are shown in Fig. 5. Whilst design number 1 appears to show the lowest value for Fe(II) concentration exiting the first settling pond this cannot be taken as a significant result since Fe(II) concentration was <1 mg/L in all cases.

3.2. Batchwise mechanical CO_2 stripping

The sites studied using the mechanical aeration and degassing technique can be split into two groups in terms of their behaviour regarding changing pH and concentrations of dissolved inorganic C species. These groups are characterised by their determination as net-acidic or net-alkaline based on the titrations carried out in the field. The changes in all of the parameters measured and described in this study showed distinct differences between the groups.

Table 2 reports the values for alkalinity, acidity, pH and Fe(II) measured at the beginning and end of the aeration experiments at each of the sites studied. For each sample, there was a range of values for pH, alkalinity, and acidity reflecting the difficulty in

Table 2
Comparison of measured hot acidity, cold acidity, alkalinity, pH, Fe(II) content, and temperature of water at the beginning and end of the batch-wise CO_2 stripping experiments.

Site	Pre-aeration					
	Hot acidity (mg/L $CaCO_3$)	Cold acidity (mg/L $CaCO_3$)	Alkalinity (mg/L $CaCO_3$)	pH	Fe(II) (mg/L)	Temperature (°C)
Blenkinsopp	33–55 net acid	423–476	264	5.6–6.0	137	13.4
Tan-y-Garn	16–22 net acid	177–186	57–58	5.6	41	12.2
Ynysarwed	29–33 net acid	259–280	143–146	5.8–5.9	93.7	13.9
Six bells	−615 net alkaline	208–222	746–752	6.6–6.7	19	18.9
Site	Post-aeration					
	Time elapsed (min)	Cold acidity (mg/L $CaCO_3$)	Alkalinity (mg/L $CaCO_3$)	pH	Fe(II) (mg/L)	Temperature (°C)
Blenkinsopp	115	21–23	34–38	5.5–5.9	5.75	17.75
Tan-y-Garn	115	16–19	1	5.5–6.0	4.3	18.0
Ynysarwed	127	45–51	5–7	5.7–5.8	2.79	18.3
Six Bells	28	0	618–631	8.4	0.05	20.0

precise measurements due to instability of pH and the imprecision of the titration end points.

The untreated waters at Blenkinsopp, Tan-y-Garn, and Ynysarwed were classified as net-acidic (positive hot acidity), and that at Six Bells was classified as net-alkaline (negative hot acidity) (Table 2).

The computed net acidity (Kirby and Cravotta, 2005a), using only data for pH, Fe(II), and alkalinity, was equivalent in sign and magnitude to the measured hot acidity. (For this computation, the concentration of Mn (not measured) was assumed to be one tenth of Fe.) Because the hot acidity excludes contributions of dissolved CO_2 (Kirby and Cravotta, 2005b), greater values for the cold acidity concentrations compared to the hot acidity indicate substantial contributions to acidity from dissolved CO_2 in the pre-aeration waters. For the net acidic waters, the Fe(II) concentration decreased to <5 mg/L after 2 h of aeration and CO_2 stripping, whereas, it decreased to <0.1 mg/L after only 30 min of aeration of the net-alkaline water (Table 2).

3.3. Evolution of chemistry with batchwise mechanical CO_2 stripping

Measured and computed changes in Fe(II) concentration using the RK4 method (Fig. 6) indicate the overall rate of Fe(II) oxidation was greater for the net-alkaline water at Six Bells than for the net-acidic waters. As a consequence of aeration, changes in pH were larger for the net-alkaline water than the net-acidic waters (Fig. 7). Changes in concentration of alkalinity and corresponding changes in HCO_3^- were comparable for both types of water, though changes in CO_3^{2-} concentration were considerably greater for the net alkaline water. After aeration, the pH of the net alkaline water had increased by almost 2 units, whereas that for the net acidic waters remained within 0.1 unit of the starting pH value. Nevertheless, the overall trends in pH were distinctive for the net acidic waters as described in the following section.

3.3.1. Net acidic waters

For the three sites that were net acidic, the initial pH values ranged from 5.6 to 5.8. It can be seen from Fig. 7 that pH increased quickly during the first 10 min of the aeration experiments due to the rapid degassing of CO_2, peaking at pH 6.3–6.5, and decreasing thereafter due to the oxidation and hydrolysis of Fe. Across all the net acidic sites, the concentration of CO_3^{2-} peaked as pH peaked and then declined again as pH dropped (Fig. 7). As would be expected over the pH range of the experiments, CO_3^{2-} concentration was several orders of magnitude lower than HCO_3^- concentration.

3.3.2. Net-alkaline waters

The pH trend for the net-alkaline water at Six Bells was very different to the net-acidic waters at the other sites (Fig. 7). During aeration and degassing of CO_2 from the water from Six Bells, pH increased from 6.7 to 8.5. The HCO_3^- concentration decreased rapidly at first corresponding to the period when Fe(II) was actively oxidised and precipitated (Eq. (6)), but gradually stabilized after Fe(II) had been depleted and this acid-producing reaction ceased. Data for the Six Bells site were only collected for 30 min as the Fe(II) oxidation rate was so high that the Fe(II) was depleted and it was not deemed necessary to continue the experiment to evaluate Fe(II) oxidation after this point. As for the net-acidic sites the trend for CO_3^{2-} concentration tracked closely that for pH. Dissolved CO_2 did not reach equilibrium with the atmosphere over the time scale of the study, an observation previously reported (Cravotta, 2007; Kirby et al., 2009). Consequently, the final steady-state pH that could be obtained with prolonged degassing of Six Bells could be greater than that reported here. On the basis of the RK4 models, at the end of the experiments for Tan-y-Garn and Ynysarwed, CO_2

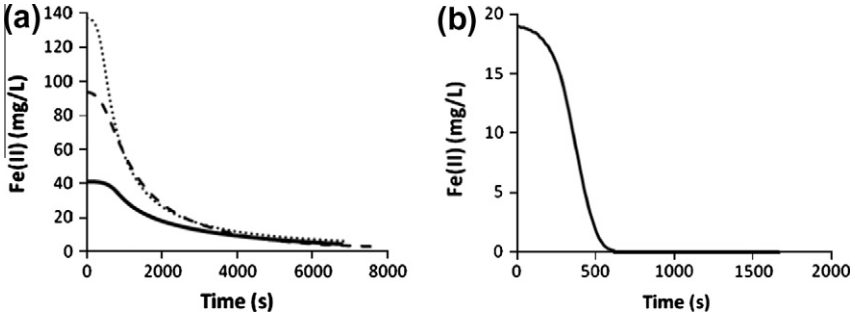

Fig. 6. Changes inFe(II) concentration during mechanical CO_2 stripping computed using the spreadsheet based RK4 model for (a) net-acid waters, Ynysarwed (dashed line, $k_1 = 1.33 \times 10^{14}\ M^{-2}\ atm^{-1}\ s^{-1}$), Blenkinsopp (dotted line, $k_1 = 8.50 \times 10^{13}\ M^{-2}\ atm^{-1}\ s^{-1}$), Tan-y-Garn (solid line, $k_1 = 2.90 \times 10^{13}\ M^{-2}\ atm^{-1}\ s^{-1}$) and (b) net-alkaline water Six Bells ($k_1 = 4.5 \times 10^{12}\ M^{-2}\ atm^{-1}\ s^{-1}$). Values of k_1 were optimised so that initial and final Fe(II) concentrations matched those measured experimentally. Values of k_1 were consistent with those given in Geroni and Sapsford (2011).

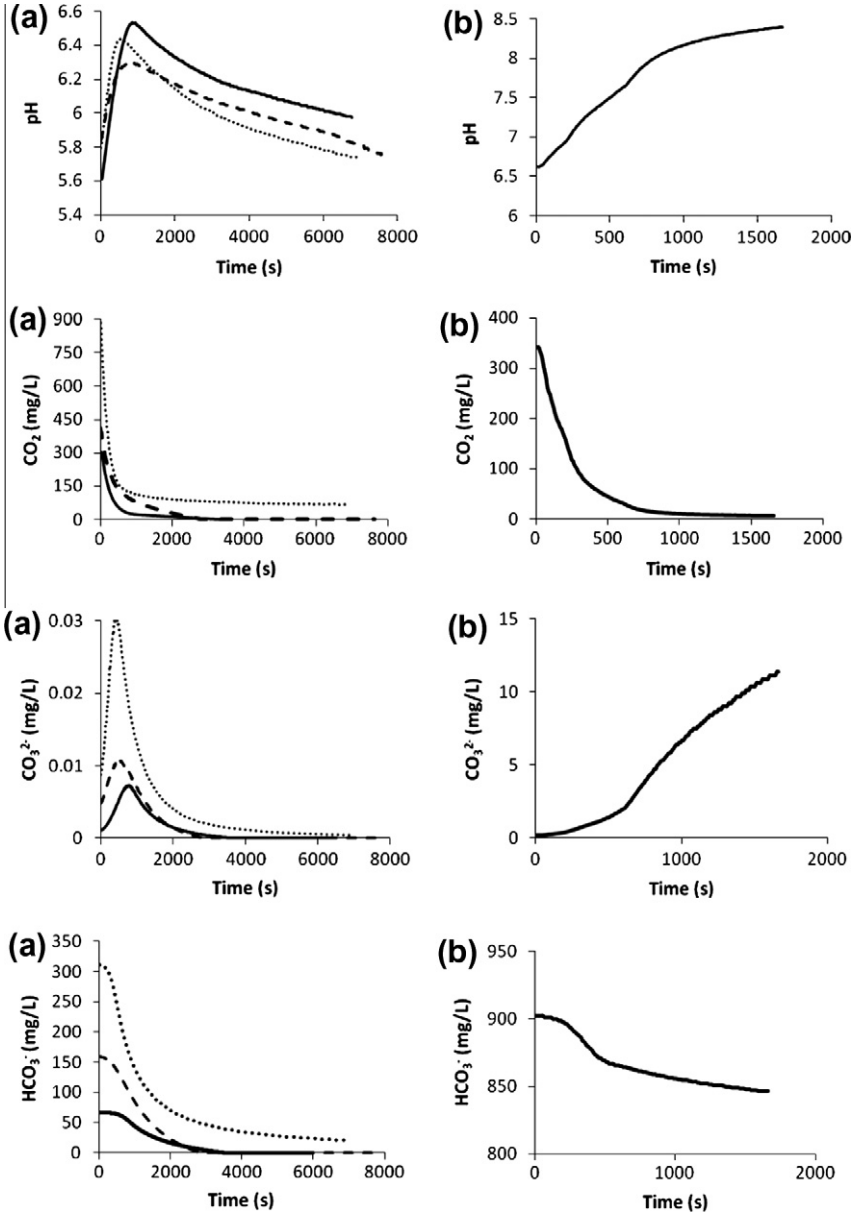

Fig. 7. Comparison of measured changes in pH and computed dissolved CO_2 species from spreadsheet based model during CO_2 stripping for (a) net acid waters, Ynysarwed (dashed line), Blenkinsopp (dotted line), Tan-y-Garn (solid line) and (b) net alkaline water, Six Bells.

concentration was predicted to decrease to zero, for Blenkinsopp 71 mg/L and for Six Bells 5 mg/L (Fig. 7).

4. Discussion

4.1. CO_2 removal

Despite having only a very short residence time (of the order of several seconds) the aeration cascades tested at Strafford proved to be effective in CO_2 stripping by removing up to 67% of dissolved CO_2. By contrast, results from the batchwise studies showed that around 3 min of mechanical aeration was required to remove a similar portion of dissolved CO_2. Since the rate of gas transfer is directly dependent on the surface area of the air water interface, it is not surprising that CO_2 degassing was more efficient with the aeration cascades. Eddies in the falling water will entrain a large number of air bubbles and encourage the formation of small droplets increasing surface area (Zhang et al., 2000), processes which will happen to a lesser extent in mechanically aerated systems. Despite this difference in efficiency, longer residence time during the mechanically aerated batchwise experiments led to larger overall changes in pH than did the aeration cascades. It should be noted that (with the exception of Tan-y-Garn) the water at Strafford contained lower initial dissolved CO_2 concentrations than the waters evaluated with the batchwise experiments with initial P_{CO_2} of approximately $10^{-0.77}$ atm compared to $10^{-0.46}$ atm at Blenkinsopp, $10^{-0.65}$ atm at Ynysarwed and $10^{-0.72}$ atm at Six Bells. Further work is required to quantify the effect of aeration cascades on water with higher initial dissolved CO_2.

The relatively small changes in pH across the aeration cascades can be accounted for by the way in which dissolved CO_2 contributes to acidity in solution. In any solution containing dissolved CO_2 there will also be H_2CO_3 present (see Eq. (4)). It is the

deprotonation of the H_2CO_3 that results in the generation of acidity and this is governed by the equilibrium expression (Eq. (8)) for Eq. (5).

$$\frac{[H^+][HCO_3^-]}{[H_2CO_3^*]} = K_1 \quad (8)$$

where $[H_2CO_3^*] = [H_2CO_3] + [CO_{2(aq)}]$. Applying the approximations that $[H^+] = [HCO_3^-]$ (i.e. ignoring autoprotolysis of water), that $[H^+] \ll [H_2CO_3^*]$ and that $[H_2CO_3] \ll [CO_{2(aq)}]$ (Stumm and Morgan, 1996) then in the case of solutions containing dissolved CO_2 (in pure water in the absence of other solutes) Eq. (8) can be reduced to Eq. (9). Thus in order to produce an increase in pH of one unit, $[CO_{2(aq)}]$ must decrease by two orders of magnitude (Eq. (10)).

$$\frac{[H^+]^2}{[CO_{2(aq)}]} = K_1 \quad (9)$$

$$pH = -\log\sqrt{K_1[CO_{2(aq)}]} \quad (10)$$

In practice this means that even with highly efficient gas transfer over an aeration cascade, there is unlikely to be sufficient residence time to degas enough CO_2 (several hundred mg/L) to produce large changes in pH. For the mechanical aeration experiments, approximately 10 min of mixing and aeration was required to change the initial pH by 1 unit.

4.2. Evolution of aqueous chemistry

4.2.1. Spreadsheet based RK4 model

The spreadsheet modelling highlighted several differences between the way in which the chemistry changes for net-acid and net-alkaline waters. The most obvious difference can be seen by comparison of the pH trends in Fig. 7. As would be expected for the net-alkaline water, the pH rises as CO_2 (and hence acidity) is lost from the system as there is sufficient alkalinity present to buffer the additional acidity generated by the formation of Fe(III) precipitates. This result for the Six Bells site is in line with other previously published studies investigating net-alkaline waters (Cravotta, 2007; Kirby et al., 2009). Generally, during aeration of net-alkaline water, the pH initially increases rapidly and then gradually approaches a steady-state value near-neutral or higher. However, the pH trends for the net-acid sites are more complex and can be explained as follows;

(1) Initial increase in pH corresponds to rapid CO_2 degassing.
(2) As rate of CO_2 degassing slows, the rate of increase of pH also slows.
(3) Rising pH (and DO) causes increasingly rapid Fe oxidation and precipitation which consumes alkalinity and causes pH to fall again.
(4) The rate of decline in pH decreases over time as Fe(II) oxidation rate decreases, partially as a result of lower Fe(II) concentrations and partly as a result of the pH dependence on the oxidation reaction.

The changes in pH in these systems are of interest not just for the removal of Fe(II) but also of a common co-contaminant Mn(II) which requires pH to be raised to at least 8.5 before oxidation and precipitation can begin to occur (Stumm and Morgan, 1996). Whilst for the net-acid sites, there is no obvious advantage in prolonged degassing, it can be seen that the pH at Six Bells had reached 8.4 by the end of the experiment and was still rising. For highly net alkaline waters, it should, therefore, be possible to remove both Fe and Mn with minimal (or even zero) chemical additions providing that sufficient CO_2 is present as HCO_3^- and CO_3^{2-} at the start and that efficient CO_2 stripping is carried out during the initial stages of treatment. In terms of the concentrations of other inorganic C species, the changes shown in Fig. 7 are what would be expected with CO_3^{2-} being present at low concentrations and HCO_3^- declining as Fe(II) declines.

One of the shortcomings of linking alkalinity consumption directly to Fe(III) precipitation was that for net-acid sites total dissolved inorganic C (TDIC) was predicted to drop to zero. In real systems, equilibration with atmospheric CO_2 would mean that TDIC would never drop to zero (H_2CO_3 will be present) and so there would always be trace amounts of carbonate species present. In order to overcome this problem, the kinetic model of CO_2 degassing, which assumed the system attained a steady-state concentration of TDIC dependent on the P_{CO_2}, was coupled with the kinetic model of Fe(II) oxidation using PHREEQCi.

4.2.2. PHREEQCi kinetic model of CO_2 degassing and Fe(II) oxidation

As with the findings of earlier studies (Geroni, 2011), CO_2 degassing during the batchwise aeration experiments was successfully modelled as a 2nd order process for inclusion with the PHREEQCi kinetics model of Fe(II) oxidation. For this model, the rate of CO_2 degassing is a direct consequence of the aeration and gas exchange and is independent of chemical interactions. The rapid, asymptotic increase in pH during early stages of aeration coincided with an asymptotic decrease in the P_{CO_2} from initial values of $10^{-0.4}$–$10^{-0.8}$ atm to estimated steady-state values of $10^{-1.7}$–$10^{-3.4}$ atm. The inverse correlation and interdependency between pH and P_{CO_2} indicates the potential for P_{CO_2} to determine pH and, hence, Fe(II) oxidation rates.

Figs. 8 and 9 show the results for measured and simulated trends in pH, Fe(II), alkalinity, and P_{CO_2} produced by coupling the rate equations for CO_2 degassing and homogeneous Fe(II) oxidation, assuming spontaneous equilibrium with atmospheric O_2, and considering the thermodynamic feasibility for precipitation of $Fe(OH)_3$. Uncalibrated and calibrated model results are displayed in Figs. 8 and 9 to indicate effects of different rate constants on model results. For reference, an uncalibrated curve for the PHREEQCi kinetics model of each experiment is displayed for the degassing of CO_2 to a steady-state P_{CO_2} of $10^{-2.8}$ atm and for the rate constant of Fe(II) oxidation equal to the reference value of $1.33 \times 10^{12}\ M^{-2}\ atm^{-1}\ s^{-1}$ (Stumm and Morgan, 1996). Generally, calibration involved iterative adjustments in the rates of CO_2 degassing and Fe(II) oxidation until a reasonable fit of the empirical data was achieved. Rather than show the average pH, which was used to estimate the rates of Fe(II) oxidation and CO_2 degassing, Fig. 8 shows the paired values of measured pH as subparallel dotted curves and corresponding estimates of the pH by selected rate models as additional curves. Because of overlap of symbols in Figs. 8 and 9, due to convergence of results during calibration, dashed curves are used to show results for the calibrated or nearly calibrated models. Since alkalinity was measured using a colorimetric indicator and did not consider other possible end points (greatest change in pH), the empirical alkalinity data were considered approximate and subject to possible adjustment. Thus, for Tan-y-Garn and Ynysarwed, the starting alkalinity values were increased from 58 to 70 mg/L and 148 to 165 mg/L, respectively, and for the calibrated Six Bells model, precipitation of calcite was simulated upon reaching supersaturation with respect to calcite according to its saturation index ($SI_{CALCITE} \leqslant 1.0$) (Table 3).

After calibration, the simulated values for pH were within the range of the paired measured values logged during the experiments, and the simulated values for Fe(II) and alkalinity were comparable to those at the beginning and end of the experiments (Figs. 8 and 9). There was general agreement between the rates of Fe(II) oxidation used for the calibrated PHREEQCi kinetics model and the spreadsheet based RK4 model (Fig. 8, Table 3). Although

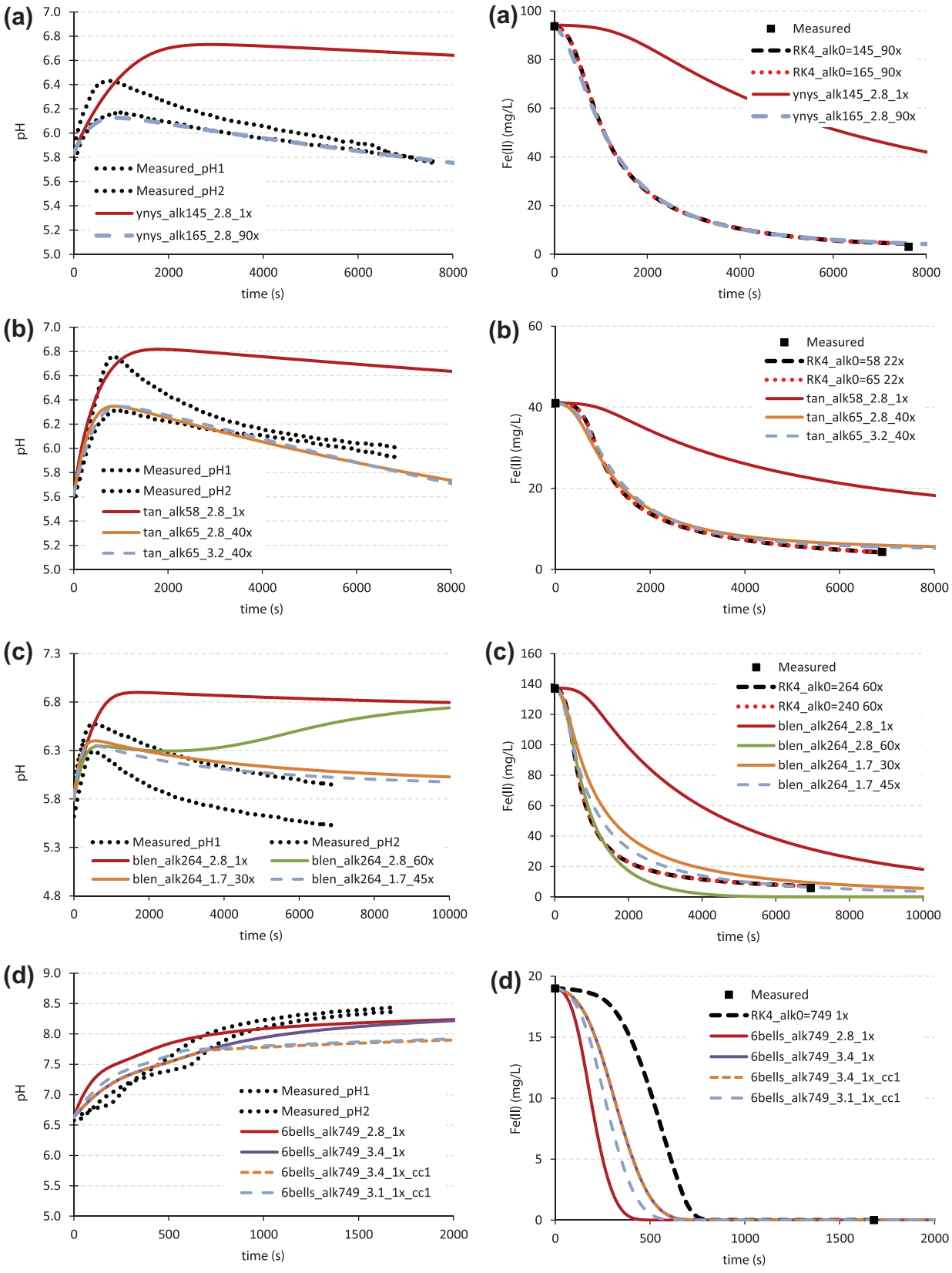

Fig. 8. Comparison of measured pH and estimated Fe(II) concentrations from spreadsheet based RK4 model to simulated pH and Fe(II) from PHREEQCi models: (a) Ynysarwed (ynys), (b) Tan-y-Garn (tan), (c) Blenkinsopp (blen), (d) Six Bells (6 bells). Values for initial alkalinity and rate constants used for the RK4 model and PHREEQCi models are summarised in Table 3. In legend, Alk_0 (58–749 mg/L $CaCO_3$ equivalent), steady-state P_{CO_2} (2.0–3.4) and k_1 multiplication factor (1–90×) are given for each simulation. Subparallel dotted lines for pH indicate the paired values measured at 10-s intervals by two pH meters during the experiments. The unbroken red curve indicates the reference simulation for values of $k_1 = 1.33 \times 10^{12}\ M^{-2}\ atm^{-1}\ s^{-1}$ and steady-state $P_{CO_2} = 2.8$.

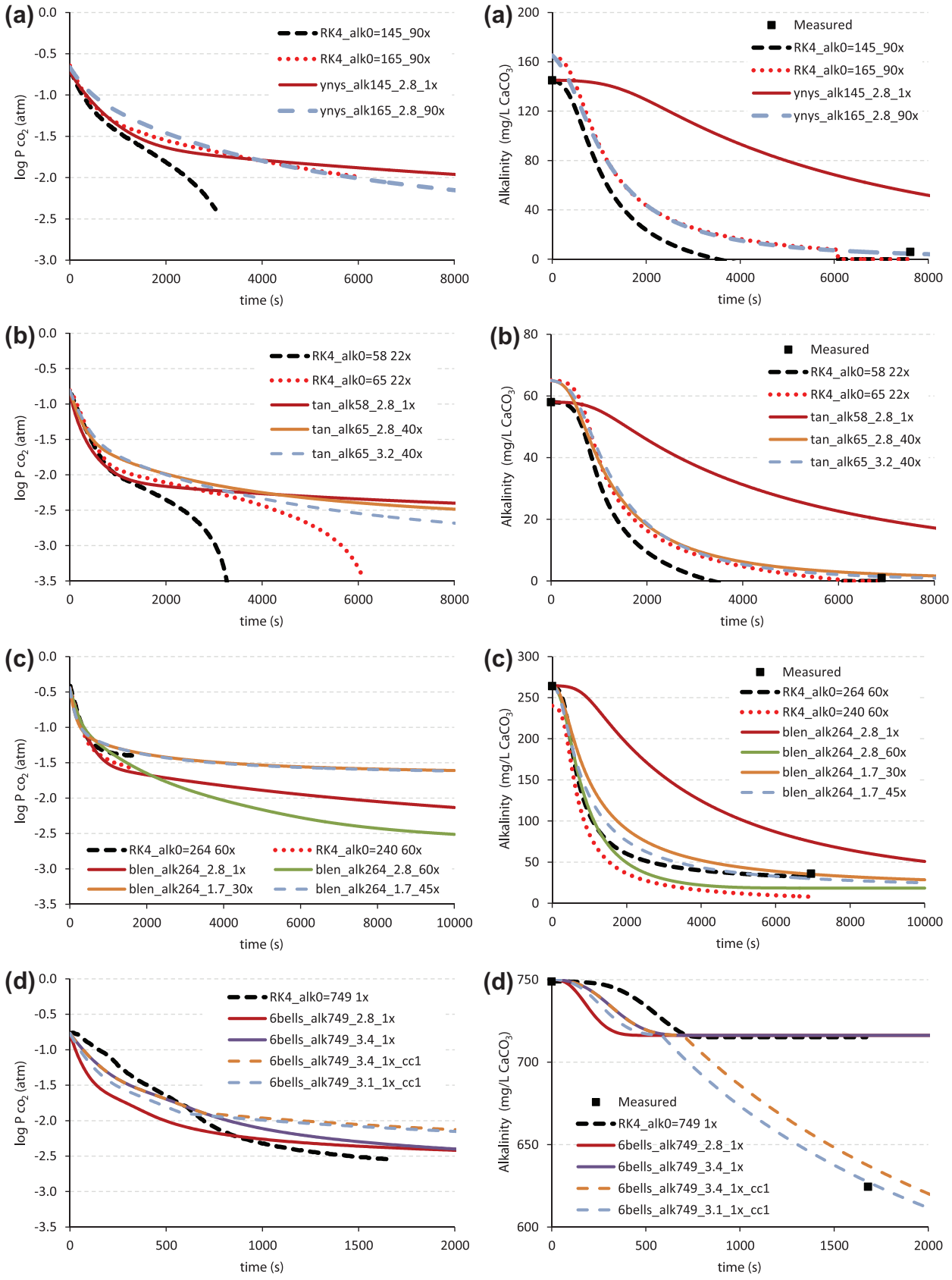

Fig. 9. Comparison of estimated P_{CO_2} and alkalinity concentrations from spreadsheet based RK4 model to simulated alkalinity and P_{CO_2} from PHREEQCi models: (a) Ynysarwed; (b) Tan-y-Garn; (c) Blenkinsopp; (d) Six Bells. Values for initial alkalinity and rate constants used for the RK4 model and PHREEQCi models are summarised in Table 3. Symbols and values for rate constants and initial conditions are given in caption for Fig. 8.

Table 3
Values of constants and associated variables used in RK4 model of Fe(II) oxidation and calibrated PHREEQCi kinetics models of CO_2 degassing and Fe(II) oxidation.

Site	k_1 factor ($k_1 = 1.33 \times 10^{12}$) RK4	$k_1^* \times 10^{12}$ at 20 °C (M^{-2} atm^{-1} s^{-1}) PHREEQCi models		Alk_0	C_o ($-\log P_{CO_2}$)	C_s ($-\log P_{CO_2}$)	k_La	Equilibrium assumption
Blenkinsopp	64–70	40	94	250	0.40	2.0	0.001417	O_2; $Fe(OH)_3$
Tan-y-Garn	22–23	20	47	70	0.80	2.8	0.000426	O_2; $Fe(OH)_3$
Ynysarwed	90–100	50	107	165	0.64	2.8	0.000203	O_2; $Fe(OH)_3$
Six Bells	1–3.4	1	1.5	749	0.77	3.1	0.000933	O_2; $Fe(OH)_3$; $CaCO_3$

For PHREEQCi models, initial pH, Fe(II), and alkalinity values and average temperature for batch aeration tests defined the starting solution. Apparent oxidation rate constant, k_1^*, for Eq. (3) indicated by the k_1 factor multiplied by 1.33×10^{12} M^{-2} atm^{-1} s^{-1}. Apparent rate constant corrected from average temperature of experiment to 20 °C using Arhhenius equation with activation energy of 23 kcal/mol (Stumm and Morgan, 1996). During kinetics simulations, exchange with atmospheric O_2 ($PO_2 = 10^{-0.27}$ atm) and precipitation of $Fe(OH)_3$ SI ⩽ 0 were specified to maintain equilibrium. For the calibrated Six Bells models, precipitation of calcite after supersaturation was considered to maintain $SI_{CALCITE} \leqslant 1.0$.

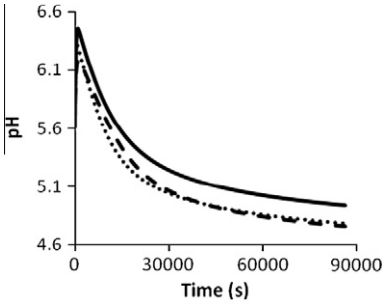

Fig. 10. Change in pH over 48 h from the kinetic PHREEQCi model for the net acid sites Ynysarwed (dashed line), Blenkinsopp (dotted line) and Tan-y-Garn (solid line).

they are not shown for the sake of brevity, trends produced for the inorganic C species also agreed closely with those estimated by the RK4 model shown in Fig. 7; however, for the net acidic waters, instead of decreasing to zero, all showed an asymptotic decay to an equilibrium value of between 1 and 3 mg/L for HCO_3^-, and between 1×10^{-5} and 5×10^{-5} mg/L for CO_3^{2-}.

By extrapolating the modelled timeframe, it is possible to estimate the final steady-state pH that would be reached once CO_2 has attained equilibrium and all Fe(II) has been oxidised or the extent of Fe(II) removal that may be anticipated for a given residence time in a treatment system. The models for the net-acid waters were run again to simulate a 48-h degassing period. The results are shown in Fig. 10, and indicate that although the rate of decrease in pH has slowed significantly, the net acidic waters are predicted to have not reached equilibrium after 2 days.

Although a consistent method was used for the batchwise mechanical aeration experiments, the estimated rates of CO_2 degassing and Fe(II) oxidation differed among the sites. Combined homogeneous and heterogeneous Fe(II) oxidation rate equations as described by Dempsey et al. (2001) as an alternative model for the PHREEQCi simulations was considered. However, the inclusion of heterogeneous oxidation did not improve the ability to simulate the empirical results. By adjusting only the apparent rate constants for homogeneous Fe(II) oxidation and CO_2 degassing, observed pH, Fe(II), and alkalinity data could be simulated. For the net alkaline water, the estimated rate of Fe(II) oxidation was identical to the reference homogeneous oxidation rate of Stumm and Morgan (1996). In contrast, to simulate the observed trends in pH and estimated Fe(II) concentrations during aeration of the net acidic water, the estimate for the oxidation rate constant was increased compared to the reference rate of 1.33×10^{12} M^{-2} atm^{-1} s^{-1} at 20 °C (Stumm and Morgan, 1996, p. 683). For these net acidic waters, values of the apparent rate constants, corrected from the average temperature during the batch experiments to a reference temperature of 20 °C using the Arrhenius equation (Table 3), with the activation energy of 23 kcal/mol (Stumm and Morgan, 1996, p. 683-684), range from 47×10^{12}–107×10^{12} M^{-2} atm^{-1} s^{-1}. These apparent oxidation rates are factors of 35–80 times greater than the reference rate value but are within the upper range of rates reported in the literature for homogeneous Fe(II) oxidation (Dempsey et al., 2001; Geroni and Sapsford, 2011). High values for the observed oxidation rates could indicate another factor(s) could be important in addition to pH and DO, such as the catalysis of Fe(II) oxidation by Fe(III) solids. Thus, the heterogeneous process may account for the increase in the apparent homogeneous oxidation rate constants for net acidic water and/or differences in rates among the sites. Nevertheless, it was not necessary to consider the more complex combined homogeneous and heterogeneous rate equations or to consider additional parameters to simulate the experimental data.

4.3. Practical implications for the treatment of ferruginous waters

One of the main aims of this work was to investigate methods for CO_2 stripping as a means to increase the efficiency and reduce the cost of treatment of ferruginous waters. The initial rapid release of excess dissolved CO_2 is what drives the changing chemistry of these ferruginous waters and as such is a critical factor in optimising Fe(II) oxidation rates in treatment systems. Within the circumneutral range, stripping CO_2 will have two impacts on mine water treatment:

(1) Raising pH and thereby raising Fe(II) (and possible Mn(II)) oxidation rate.
(2) Reducing the quantities of alkali required to raise pH.

For net-alkaline waters stripping CO_2 will raise pH and result in higher Fe(II) oxidation rates which has the potential to reduce the area required for treatment (up to the point where settling of the resulting Fe(III) precipitates becomes the rate limiting step). For net-acid waters where active treatment such as lime dosing to raise pH is required, stripping CO_2 can dramatically reduce the quantities of alkali required. A change in dissolved CO_2 of 120 mg/L corresponds to a reduction in the quantity of lime required to neutralise the associated carbonic acid of 202 mg/L. At a treatment site where the flow rate is 50 L/s this gives a reduction of 864 kg of lime per day. Not only does this provide a benefit in economic terms as a reduction in the up-front purchase cost of the reagent, but a lower concentration of dissolved $CaCO_3$ will result in less lime scale formation reducing maintenance costs and a reduced mass of sludge that must be disposed. Likewise, pre-aerating ferruginous water to remove Fe(II) may be effective to decrease

the risk for armouring of limestone in passive treatment systems; decreased pH of net acidic water, resulting from Fe(III) hydrolysis, may increase the rate of limestone dissolution (Cravotta, 2007, 2008).

Of the two methods of CO_2 degassing described in this paper, the aeration cascade seems to be the best option in terms of cost/benefit for inclusion in treatment systems for ferruginous waters. Experience suggests that many net-alkaline treatment systems are likely to be limited by settling rates of Fe(III) precipitates (Sapsford and Pugh, 2010), so increasing pH beyond what can be achieved with aeration cascades is unlikely to make significant reductions in treatment footprint (without some method of increasing settling rate). Furthermore, forced aeration actually may prevent or reduce settling rates of newly formed particles.

In the case of net-acidic waters, whilst forced aeration used during the batch experiments did result in accelerated removal of nearly all dissolved Fe(II) and CO_2, the cost of building and maintaining such a system in the long term could be orders of magnitude greater than for an aeration cascade. Furthermore, adequate hydraulic head may not be available for aeration cascades at all sites. For net-acidic waters, the balance must be struck between the residence time and cost requirements of forced aeration versus the savings that can be realised from reduced lime consumption.

5. Conclusions

This study has shown that both aeration cascades and forced mechanical aeration can be effective in stripping dissolved CO_2 from circumneutral ferruginous waters. The rate of loss of dissolved CO_2 was higher for the aeration cascades despite a residence time of the order of several seconds; more CO_2 was stripped overall during mechanical aeration (leading to greater pH changes). The efficient removal of CO_2 by aeration cascades is attributed to the expansive air–water interface and the relatively rapid rate of CO_2 loss during early stages of aeration. The design of the aeration cascade had little effect on the amount of CO_2 stripped from the water, and it appears that for cascades of the same height a single waterfall is as effective in removing CO_2 as a stepped cascade both with and without plunge pools.

Degassing of CO_2 was shown to have a major influence on the pH and associated Fe(II) oxidation rates for all of the sites studied. Removal of CO_2 caused an increase in pH of nearly 2 units for the net-alkaline water which would result in an acceleration of Fe(II) oxidation rate of 4 orders of magnitude. For the net-acidic sites, stripping CO_2 caused an initial increase in pH and subsequently allowed pH levels to remain high enough for Fe(II) levels to be reduced from a maximum of 140 mg/L to <5 mg/L within 2 h.

The rate of CO_2 degassing was successfully described using a 2nd order asymptotic exponential model and that for Fe(II) oxidation was described using a 1st order exponential rate model for homogeneous oxidation. Based on reported values in the literature, estimates for the rates of CO_2 degassing and Fe(II) oxidation were considered to simulate observed data on pH (measured continuously) and the initial and final Fe(II) and alkalinity values. With the modelling approach used, the pH was treated as a master variable controlled mainly by the rate of CO_2 degassing and secondarily by the rate of Fe(II) oxidation. The empirical data and associated simulations indicated that hydrolysis of Fe(III) generated by the latter process depressed the pH of net acidic water to a greater extent than that of net alkaline water.

Although limited by the availability and quality of time-series data, the kinetics modelling provided insight into the interactions among chemical processes and the relative importance of specific parameters. Empirical data on temperature, DO, pH, alkalinity, Fe(II) concentration, and associated solutes and solids generally are needed to characterise the chemical evolution of poorly buffered ferruginous water and to refine the kinetics of CO_2 degassing and Fe(II) oxidation during the course of aeration tests or within treatment systems. Given the strong dependency of Fe(II) oxidation on pH and temperature, serial data on these parameters are essential for evaluating the kinetics of Fe(II) oxidation—pH measurements that are accurate to ±0.1 units could be achieved by use of new, high-quality electrodes. Likewise, the pH and initial alkalinity concentration data are essential for estimation of initial TDIC and rate of CO_2 degassing—alkalinity measured to an alternative pH endpoint (greatest rate of change) could be more accurate than its measurement using a colorimetric indicator. Serial measurements of Fe(II) and total Fe during the aeration experiments could be helpful to evaluate the importance of homogeneous and heterogeneous oxidation rate models. With accurate information and refined models, the interdependency of pH, CO_2 degassing, and Fe(II) oxidation rates on mine water evolution can be evaluated to optimise treatment strategies for ferruginous waters.

Acknowledgements

The authors would like to thank the UK Coal Authority, EPSRC, and Cardiff University for their financial support of the project. Helpful comments on the draft manuscript were provided by Carl S. Kirby and two anonymous reviewers. Any use of trade, firm, or product names is for descriptive purposes only and does not imply endorsement by the U.S. Government.

References

American Public Health Association (APHA), 1998. Standard Methods for the Examination of Water and Wastewater, 20th ed. American Public Health Association, Washington, DC.

Carter, R.C., Tyrrel, S.F., Howsam, P., 1996. Strategies for Handpump water supply programmes in less-developed countries. Water Environ. J. 10, 130–136.

Coulton, R., Bullen, C., Hallett, C., 2003. The design and optimisation of active mine water treatment plants. Land Contam. Reclam. 11, 273–279.

Cravotta III, C.A., 2007. Passive aerobic treatment of net-alkaline, iron laden drainage from a flooded underground anthracite mine, Pennsylvania, USA. Mine Water Environ. 26, 128–149.

Cravotta III, C.A., 2008. Laboratory and field evaluation of a flushable oxic limestone drain for treatment of net-acidic, metal-laden drainage from a flooded anthracite mine, Pennsylvania, USA. Appl. Geochem. 23, 3404–3422.

Dempsey, B.A., Roscoe, H.C., Ames, R., Hedin, R., Jeon, B.-H., 2001. Ferrous oxidation chemistry in passive abiotic systems for the treatment of mine drainage. Geochem. Explor. Environ. Anal. 1, 81–88.

DeNicola, D.M., Stapleton, M.G., 2002. Impact of acid mine drainage on benthic communities in streams: the relative roles of substratum vs. aqueous effects. Environ. Pollut. 119, 303–315.

Faust, S.D., Osman, M.A., 1998. Chemistry of Water Treatment, second ed. Ann Arbor Press.

Geroni, J.N., 2011. Rates and Mechanisms of Chemical Processes Affecting the Treatment of Ferruginous Mine Water. Cardiff School of Engineering, Cardiff. Ph.D. Thesis.

Geroni, J.N., Sapsford, D.J., 2011. Kinetics of iron (II) oxidation determined in the field. Appl. Geochem. 26, 1452–1457.

Geroni, J.N., Sapsford, D.J., Barnes, A., Watson, I.A., Williams, K.P., 2009. Current performance of passive treatment systems in South Wales UK. In: Proc. Internat. Mine Water Conf., 19–23 October, Pretoria, South Africa.

Jarvis, A.P., England, A., Mee, S., 2003. Mine water treatment at Six Bells colliery, South Wales: problems and solutions, from conception to completion. Land Contam. Reclam. 11, 153–160.

Kirby, C.S., Cravotta, C.A., 2005a. Net alkalinity and net acidity 1: Theoretical considerations. Appl. Geochem. 20, 1920–1940.

Kirby, C.S., Cravotta, C.A., 2005b. Net alkalinity and net acidity 2: Practical considerations. Appl. Geochem. 20, 1941–1964.

Kirby, C.S., Dennis, A., Kahler, A., 2009. Aeration to degas CO_2, increase pH, and increase iron oxidation rates for efficient treatment of net alkaline mine drainage. Appl. Geochem. 24, 1175–1184.

Kothari, N., 1988. Groundwater, iron and manganese an unwelcome trio. Water Eng. Manag. 135 (2), 25–26.

Langmuir, D., 1997. Aqueous Environmental Geochemistry. Prentice Hall, New Jersey, USA.

Larson, T.E., Buswell, A.M., 1942. Calcium carbonate saturation index and alkalinity interpretations. J. Am. Water Works Assoc. 34, 1667–1684.

Lucassen, E.C.H.E.T., Smolders, A.J.P., Roelofs, J.G.M., 2000. Increased groundwater levels cause iron toxicity in *Glyceria fluitans* (L.). Aquat. Bot. 66, 321–327.

Moncur, M.C., Jambor, J.L., Ptacek, C.J., Blowes, D.W., 2009. Mine drainage from the weathering of sulphide minerals and magnetite. Appl. Geochem. 24, 2362–2373.
Nordstrom, D.K., 2011. Hydrogeochemical processes governing the origin, transport and fate of major and trace elements from mine wastes and mineralized rock to surface waters. Appl. Geochem. 26, 1777–1791.
Parkhurst, D.L., Appelo, C.A.J., 1999. User's Guide to PHREEQC (Version 2) – A Computer Program for Speciation, Batch-reaction, One-dimensional Transport, and Inverse Geochemical Calculations, U.S. Geol. Sur. Water-Resour. Invest. Rep. 99-4259.
PIRAMID, 2003. Engineering Guidelines for the Passive Remediation of Acidic and/or Metalliferous Mine Drainage and Similar Wastewaters. University of Newcastle upon Tyne, ISBN 0-9543827-1-4.
Rose, A.W., Cravotta III, C.A., 1998. Geochemistry of coal-mine drainage. In: Brady, K.B.C., Smith, M.W., Schueck, J.H. (Eds.), The Prediction and Prevention of Acid Drainage from Surface Coal Mines in Pennsylvania. Pennsylvania Dept. of Environmental Protection, Harrisburg.
Sapsford, D.J., Pugh, D., 2010. Evaluation of Physicochemical Processes Occurring in Mine Water Treatment Systems in South Wales, UK. Technical Report to Coal Authority Cardiff School of Engineering Report No: 3200.
Stumm, W., Lee, G.F., 1961. Oxygenation of ferrous iron. Ind. Eng. Chem. 53, 143–146.
Stumm, W., Morgan, J.J., 1996. Aquatic Chemistry, Chemical Equilibria and Rates in Natural Waters, third ed. Wiley Interscience.
Younger, P.L., Banwart, S.A., Hedin, A.S., 2002. Minewater: Hydrology, Pollution, Remediation. Springer.
Zhang, D.D., Peart, M., Zhang, Y.-J., Zhu, A., Cheng, X., 2000. Natural water softening processes by waterfall effects in karst areas. Desalination 129, 247–259.